Fluorescence spectroscopy of UV-MALDI matrices and implications of ionization mechanisms

Hou-Yu Lin, Hsu Chen Hsu, I-Chung Lu, Kuo-Tung Hsu, Chih-Yu Liao, Yin-Yu Lee, Chien-Ming Tseng, Yuan-Tseh Lee, and Chi-Kung Ni

Citation: The Journal of Chemical Physics **141**, 164307 (2014); doi: 10.1063/1.4898372
View online: http://dx.doi.org/10.1063/1.4898372
View Table of Contents: http://scitation.aip.org/content/aip/journal/jcp/141/16?ver=pdfcov
Published by the AIP Publishing

Fluorescence spectroscopy of UV-MALDI matrices and implications of ionization mechanisms

Hou-Yu Lin,[1,a)] Hsu Chen Hsu,[1] I-Chung Lu,[1] Kuo-Tung Hsu,[2] Chih-Yu Liao,[2] Yin-Yu Lee,[2] Chien-Ming Tseng,[3] Yuan-Tseh Lee,[1,a)] and Chi-Kung Ni[1,b)]
[1]*Institute of Atomic and Molecular Sciences, Academia Sinica, Taipei 10617, Taiwan*
[2]*National Synchrotron Radiation Research Center, Hsinchu 30076, Taiwan*
[3]*Department of Applied Chemistry, National Chiao Tung University, Hsinchu 30010, Taiwan*

(Received 11 August 2014; accepted 6 October 2014; published online 24 October 2014)

Matrix-assisted laser desorption ionization (MALDI) has been widely used in the mass analysis of biomolecules; however, there are a lot of debates about the ionization mechanisms. Previous studies have indicated that S_1-S_1 annihilation might be a key process in the generation of primary ions. This study investigates S_1-S_1 annihilation by examining the time-resolved fluorescence spectra of 12 matrices. No S_1-S_1 annihilation was observed in six of these matrices (3-hydroxy-picolinic acid, 6-aza-2-thiothymine, 2,4-dihydroxy-acetophenone, 2,6-dihydroxy-acetophenone, 2,4,6-trihydroxy-acetophenone, and ferulic acid). We observed two matrix molecules reacting in an electronically excited state (S_1) in five of these matrices (2,5-dihydroxybenzoic acid, α-cyano-4-hydroxycinnamic acid, 2,5-dihydroxy-acetophenone, 2,3-dihydroxybenzoic acid, and 2,6-dihydroxybenzoic acid), and S_1-S_1 annihilation was a possible reaction. Among these five matrices, no S_1-S_1 annihilation was observed for 2,3-dihydroxybenzoic acid in typical peak power region of nanosecond laser pulses in MALDI, but a very small value of reaction rate constant was observed only in the high peak power region. The excited-state lifetime of sinapinic acid was too short to determine whether the molecules reacted in an electronically excited state. No correlation was observed between the ion generation efficiency of MALDI and S_1-S_1 annihilation. The results indicate that the proposal of S_1-S_1 annihilation is unnecessary in MALDI and energy pooling model for MALDI ionization mechanism has to be modified. © *2014 AIP Publishing LLC*. [http://dx.doi.org/10.1063/1.4898372]

I. INTRODUCTION

Matrix-assisted laser desorption ionization (MALDI)[1,2] has been widely used for the mass analysis of biomolecules. MALDI involves mixing an analyte with a suitable matrix to form a solid mixture. When ultraviolet (UV) laser pulses at wavelengths of 337 or 355 nm and pulse durations of 2–7 ns irradiate on a sample, a large quantity of analyte and matrix molecules (ions and neutrals) are released. These ions are subsequently analyzed using a mass spectrometer. Although MALDI was invented more than 20 years ago, there are a lot of debates about the ionization mechanisms.[3–12]

The energy pooling model has been applied to explain the generation of the primary ions.[7,8] According to the model, molecules in highly electronically excited singlet state results from annihilation between two molecules in the first electronically excited singlet state (i.e., S_1-S_1 annihilation). The primary ions are generated by the subsequent annihilation between one molecule in the first electronically excited singlet state, and the other in a highly electronically excited singlet state (S_1-S_n annihilation), or by thermal ionization from S_n.

Ehring and Sundqvist[13] first proposed that a relationship exists between the S_1-S_1 annihilation and the ion-generation mechanism in MALDI. They demonstrated that the fluorescence quantum yield of 2,5-dihydroxybenzoic acid (2,5-DHB) decreases as laser fluence increases, presumably because of the S_1-S_1 annihilation. Hillenkamp and co-workers employed a similar method to investigate the fluorescence quantum yields of 2,5-DHB, 2-aminobenzoic acid, and 3-hydroxypicolinic acid (3-HPA).[14] They considered both S_1-S_1 annihilation and two-photon absorption as potential pathways for decreasing the fluorescence quantum yields. They conducted numerical simulations, reporting that the simulation based on S_1-S_1 annihilation provided a closer fit to their experimental data than the simulation based on two-photon absorption.

Based on the S_1-S_1 annihilation concept, Knochenmuss developed a numerical model, namely energy pooling, for quantitatively describing the ion-generation process in MALDI.[7,8] However, our recent report[15] pointed out that the aforementioned studies failed to distinguish between the ion yields of matrices and analytes. Based on the model proposed by Knochenmuss, which involved using a 355 nm laser pulse for molecular excitation, the ion yield of matrices is approximately 10^4-fold more than the results of many experimental measurements.[15–18] Knochenmuss's prediction is close to only one experimental measurement, which involved using a 193 nm laser pulse.[19]

Molecules must satisfy several properties to undergo S_1-S_1 annihilation. First, an appropriate interaction must

[a)] Also at Department of Chemistry, National Taiwan University, Taipei 10617, Taiwan.
[b)] Also at Department of Chemistry, National Tsing Hua University, Hsinchu 30013 Taiwan.

occur between an energy donor and accepter. Second, to accept energy from the donor, the energy acceptor must have an electronically excited state (S_n) located at an appropriate energy level. Finally, competing processes such as photon emissions, internal conversions, or other reactions involving molecules in the excited states (S_1 and S_n) must be slow. Annihilation usually occurs in the triplet-states because of the relatively long lifetime of the triplet states.[20]

The rate equation for the population of molecules in the S_0 and S_1 states under laser irradiation can be expressed as follows:

$$\frac{d[S_0(t)]}{dt} = -I(t)\alpha_0[S_0(t)] + I(t)\alpha_{0s}[S_1(t)] + k_1[S_1(t)] + k_2[S_1(t)]^2, \quad (1)$$

$$\frac{d[S_1(t)]}{dt} = I(t)\alpha_0[S_0(t)] - I(t)\alpha_{0s}[S_1(t)] - I(t)\alpha_1[S_1(t)] + I(t)\alpha_{1s}[S_n(t)] - k_1[S_1(t)] - 2k_2[S_1(t)]^2, \quad (2)$$

where α_0 denotes the absorption cross section from the ground state, S_0, to the first excited singlet state S_1; α_1 represents the absorption cross section from the S_1 state to the higher singlet state, S_n; α_{0s} is the stimulated emission cross section from the S_1 state to the S_0 state; α_{1s} is the stimulated emission cross section from the S_n state to the S_1 state; $I(t)$ represents the laser intensity at time t; and k_1 and k_2 denote the reaction rate constants of the first-order reactions (e.g., photon emission, internal conversion) and second-order reactions (e.g., S_1-S_1 annihilation), respectively.

Fluorescence quantum yield Q is proportional to the integration of $S_1(t)$ from the beginning of a laser pulse (i.e., $t = 0$) until the fluorescence intensity decays completely (i.e., $t = t'$).

$$Q = C \times \int_{t=0}^{t=t'} S_1(t)dt, \quad (3)$$

where C is the proportional constant. The calculations of quantum yields from $S_1(t)$ involve parameters α_0, α_1, α_{0s}, and α_{1s}, as shown in Eq. (2). Previous studies have employed the fluorescence quantum yield to investigate S_1-S_1 annihilation. Because various parameters of excited state in Eq. (2) are unknown, uncertainties exist in quantum yield calculations. As a result, fluorescence quantum yield is not the optimal method for investigating S_1-S_1 annihilation.

Equation (2) can be simplified to Eq. (4) when laser intensity completely decays to zero:

$$\frac{d[S_1(t)]}{dt} = -k_1[S_1(t)] - 2k_2[S_1(t)]^2. \quad (4)$$

Equation (4) can be used to describe the fluorescence intensity decay when the excitation laser pulse width is much shorter than the excited state lifetime and the fluorescence intensity is measured after the excitation laser pulse finishes.

In a recent study,[21] we investigated S_1-S_1 annihilation and measured the time-resolved fluorescence intensities of two commonly used matrices (2,4,6-trihydroxyacetophenone (THAP) and 2,5-DHB) by using a short laser pulse (20 ps) and high time resolution detector (1 ps). We demonstrated that no S_1-S_1 annihilation occurred in THAP, indicating that S_1-S_1 annihilation is not essential to the ion-generation processes in MALDI. This study replicates the method employed in our previous study to investigate S_1-S_1 annihilation of 12 matrices. Nine of these matrices were commonly used MALDI matrices at 337 and 355 nm laser wavelengths, as listed by Hillenkamp and Karas.[22] The results indicated that S_1-S_1 annihilation does not occur in most matrices. Furthermore, the ion-generation efficiency exhibited no correlation with S_1-S_1 annihilation efficiency, indicating that S_1-S_1 annihilation is not a major ionization mechanism of MALDI.

II. EXPERIMENTAL METHOD

Solid state matrices were placed in a vacuum (1×10^{-6} Torr), and their fluorescence spectra were measured using a spectrograph combined with a time-gated intensified charge-coupled device (ICCD) detector (Shamrock 303i and DH340T-18U-73 ICCD, Andor Technology). The third harmonic of a Nd:YAG laser (355 nm, 5 ns pulse duration, Minlite II, Continuum) was used for molecular excitation. Figure 1 shows a schematic diagram of the apparatus.

The time-resolved fluorescence intensity was measured using the third harmonic of a Nd:YAG laser (355 nm, <20 ps pulse duration, PL2210D-1K-P20, Ekspla, Lithuania, manually operated at about 1 Hz) to excite the samples, and the fluorescence was detected using a streak camera (1 ps time resolution, C10910-S21, Hamamatsu Photonics K. K., Japan). Figure 2 shows the schematic diagram of the apparatus used in the time-resolved fluorescence intensity measurements. The average full width at half maximum of the 355-nm laser pulses was approximately 30 ps, including the effects of instrument response and time jitter of the laser pulse.

To measure the fluorescence spectra and time-resolved fluorescence intensity, we employed a rotatable sample-holder similar to that reported in our previous study.[23] A stainless steel cylindrical sample-holder (10 mm diameter) was positioned inside the vacuum chamber, which was evacuated

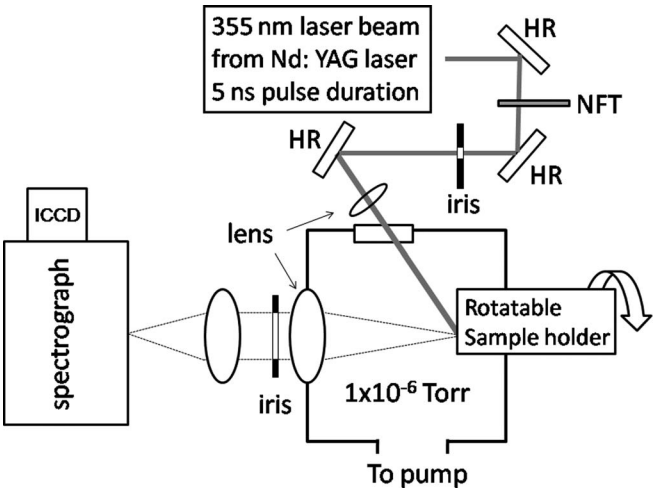

FIG. 1. Schematic diagram of the apparatus for measuring fluorescence spectra. HR: a mirror with high reflectivity at 355 nm, NFT: a step-variable metallic neutral density filter (Thorlabs, model: NDC-100S-4M).

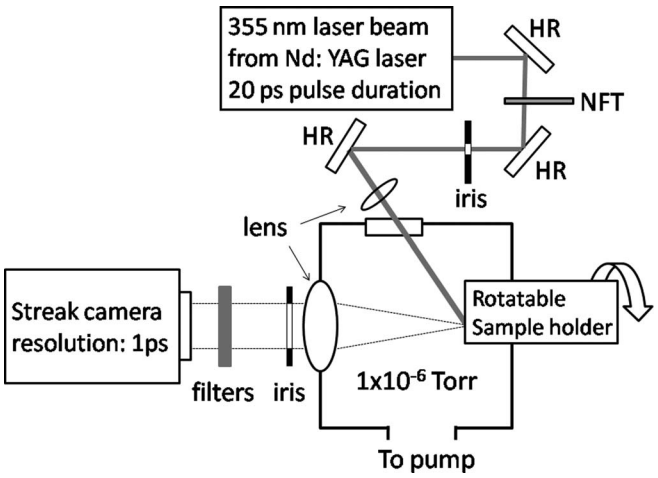

FIG. 2. Schematic diagram of the time-resolved fluorescence experimental design. The filters include a dielectric coated mirror exhibiting high reflectivity for wavelengths shorter than 360 nm, and a high-transmission color filter for wavelengths longer than 385 nm.

using a turbo molecular pump to maintain constant pressure (approximately 1×10^{-6} Torr). The laser irradiation spot on the sample surface was located on the central axis of the lens, but the rotation axis of the sample-holder was offset 4 mm from the central axis of the lens. Thus, the sample surface could be replaced after firing several laser shots by rotating the sample holder without breaking the vacuum.

The MALDI grade materials were used in fluorescence lifetime measurement. If MALDI grade materials were not commercially available, high purity material (99% or 98%) was purchased and recrystallized twice before use. Some non-MALDI grade materials were used directly without further purification for the comparison to MALDI grade materials. Most of the materials were purchased from Sigma Aldrich, some of them were from Acros Organics. Details of these materials were described in the supplementary material.[24]

The samples were prepared using the dried droplet method. A stock solution was prepared for each matrix by dissolving the corresponding compounds in 50% acetonitrile aqueous solution. Subsequently, the solution was placed on the sample-holder and vacuum-dried. This process was repeated until the thickness of the solid sample (after vacuum-drying) was approximately 0.5 mm.

Each spectrum or data point reported in this study represents the average of 3–10 measurements at each level of laser fluence. The number of measurements depended on the signal-to-noise ratio. Each measurement represents the accumulation of 10 (large laser fluence) to 200 laser shots (small laser fluence). Fresh samples were used for each measurement.

III. METHOD OF DATA ANALYSIS

When the laser fluence is small (i.e., when $S_1(t)$ is small), the second term on the right side of Eq. (4) is negligible. Fluorescence intensity decay can be described as a single exponential decay. As the laser fluence increases, the second term begins contributing in Eq. (4) if k_2 is not small. Consequently, the time-resolved fluorescence intensity deviates from a single exponential decay. Comparing the fluorescence intensity decay at a high level of laser fluence with the numerical calculations of a single exponential decay provides a sensitive method for determining whether S_1-S_1 annihilation occurs.

An accurate k_2 value can be determined from the fits of numerical simulations according to Eqs. (1) and (2) to experimental measurements. Regarding the numerical simulations, each sample was divided into 20-nm-thick layers. The depth of each layer was sufficiently small to ensure that laser fluence does not change very much from the top to the end of the layer. For each layer, numerical simulations were calculated in one-picosecond increments. The final results are expressed as the summation of all layers.

IV. RESULTS AND DISCUSSION

In this study, we found that the lifetime of the excited state was considerably shorter than the duration of the nanosecond laser pulse used in typical MALDI experiments. To ensure the populations of molecules in the S_1 state, $S_1(t)$, in this study are similar to the populations in typical MALDI experiments, the peak power of the 20 ps laser pulse used in this work must be identical to that of the nanosecond laser pulse used in typical MALDI experiments. The rate constant k_2 obtained under this condition would be representative of the rate constant k_2 in typical MALDI experiments. In typical MALDI experiments involving nanosecond laser pulses from the third harmonic of an Nd:YAG laser, the laser pulse width and fluence range from 5 to 7 ns and 50 to 500 J/m^2, respectively. The peak power of laser fluence between 0.2 and 2 J/m^2 for a 20 ps laser pulse width is similar to the typical peak power of nanosecond laser pulses in MALDI. The laser fluence applied in this study not only covered the range from 0.2 to 2 J/m^2 but also extended to a wider range. At high laser fluences, $S_1(t)$ is large; consequently, Eq. (4) becomes much more sensitive for determining whether S_1-S_1 annihilation occurs.

As we described in text below, lifetimes are in the range from subpicosecond to subnanosecond. They are much shorter than the duration of desorption process. The fluorescence obtained in this work represents the fluorescence of molecules in solid state.

A. Nine commonly used UV-MALDI matrices

1. 2,5-Dihydroxybenzoic acid (2,5-DHB)

Figure 3(a) shows the fluorescence spectra of solid state matrices after the excitation by 355 nm photons. Figure 3(b) shows the time-resolved fluorescence intensities of 2,5-DHB at various laser fluences. At ultra-low laser fluences (0.03 J/m^2), the fluorescence intensity (proportional to the excited state population, $S_1(t)$) can be expressed as a single exponential function of an excited-state lifetime $\tau = 1/k_1 = 625$ ps. This lifetime represents the decay of $S_1(t)$ through only photon emission, internal conversion, and intersystem crossing. As the laser fluence increased, the excited-state lifetime decreased. The fluorescence intensity at high laser fluence can be described using Eq. (4), indicates that two

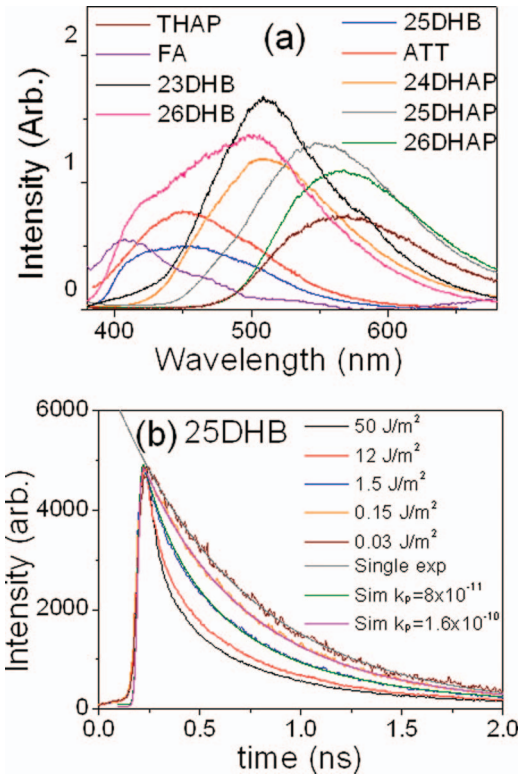

FIG. 3. (a) Fluorescence spectra of various solid matrices, using a 5-ns laser pulse (355 nm) for excitation and spectrograph/ICCD for detection. The time-gated window of ICCD was opened 10 ns before the excitation laser pulse arrived, and it remained open for 100 ns. (b) Time-resolved fluorescence intensity of 2,5-DHB at various laser fluences. A 20-ps laser pulse (355 nm) was used for excitation and a streak camera (1 ps resolution) was used for detection. The fluorescence intensities at various laser fluences were multiplied by different factors so that they have the same maximum intensity.

excited molecules reacted, and that one of the reactions might be attributable to S_1-S_1 annihilation. The value of k_2 was obtained from the fit of numerical simulations using Eqs. (1) and (2) to experimental data. The accuracy of k_2 depends on the accuracy of parameters α_0, α_1, α_{0s}, and α_{1s}. Only the absorption cross section, α_0, has been reported (9×10^4 cm^{-1} or 1.6×10^{-17} cm^2 for a density of 1.43 g/cm^3).[25] The values of the other parameters are not known. However, k_2 is less sensitive to α_1, α_{0s}, and α_{1s} at low laser fluences because the corresponding multiphoton absorption and stimulated emission do not make big contribution in Eq. (2). The reaction rate constant k_2 obtained from the fit of numerical simulation to the experimental data at low laser fluence (0.15 J/m^2), was 1.6×10^{-10} cm^3 molecule^{-1} s^{-1}. The plots of logarithm of fluorescence intensity verse time are shown in the supplementary material.[24] The non-MALDI grade material shows similar results. The values are listed in Table I.

2. α-Cyano-4-hydroxycinnamic acid (CHCA)

Hoyer *et al.* reported the change of fluorescence spectra of CHCA after illumination by 325 nm photons.[26,27] The initial fluorescence spectra exhibited a broad band from 430 to 700 nm, and the maximum intensity was observed at 500 nm. After illuminating the CHCA by 325 nm photons (4 MHz, 100 pJ per pulse in 100 μm spot size) for 200 to 600 s, the fluorescence spectra exhibited an additional broad band from 450 to 700 nm which the maximum intensity was observed at 560 nm. The additional broad band was attributed to fluorescence from photodimers that were products of the reaction between one molecule in the S_1 state and one molecule in the

TABLE I. Rate constants k_1 and k_2 for various matrices.

Matrix	k_1 (s^{-1})	k_2 (cm^3 molecule^{-1} s^{-1})	
2,5-DHB[a]	1.6×10^9	1.6×10^{-10}	
2,5-DHB[b]	1.7×10^9	1.2×10^{-10}	
CHCA[a]	1.73×10^{10}	1.7×10^{-10}	
CHCA[b]	2.1×10^{10}	2.5×10^{-10}	
SA[a]	9.5×10^{10}	not determined	
SA[b]	1.2×10^{11}	not determined	
3-HPA[a]	1.2×10^{10}	$<5 \times 10^{-13}$[c]	no S_1-S_1 annihilation observed
ATT[a]	1.9×10^{10}	$<6 \times 10^{-12}$[c]	no S_1-S_1 annihilation observed
2,4-DHAP[a]	9.1×10^8	$<3 \times 10^{-14}$[c]	no S_1-S_1 annihilation observed
2,4-DHAP[b]	9.1×10^8	$<5 \times 10^{-14}$[c]	no S_1-S_1 annihilation observed
2,5-DHAP[a]	3.58×10^9	6×10^{-12}[c]	
2,6-DHAP[a]	1.85×10^{10}		no S_1-S_1 annihilation observed
	3.3×10^9		
THAP[a]	8.3×10^9	$<1 \times 10^{-12}$[c]	no S_1-S_1 annihilation observed
THAP[b]	$5.7–9 \times 10^9$	$<5 \times 10^{-13}$[c]	no S_1-S_1 annihilation observed
FA[a]	9.6×10^9	$<2 \times 10^{-13}$	no S_1-S_1 annihilation observed
FA[b]	9.5×10^9	$<1 \times 10^{-13}$	no S_1-S_1 annihilation observed
2,3-DHB[a]	2.5×10^9	5×10^{-13}[c]	S_1-S_1 annihilation observed only at very high laser fluence
2,3-DHB[b]	2.5×10^9	$<2 \times 10^{-13}$[c]	no S_1-S_1 annihilation observed
2,6-DHB[a]	2.1×10^9	3.2×10^{-11}[c]	
2,6-DHB[b]	2.8×10^9	6×10^{-11}[c]	

[a]MALDI grade material or recrystallized twice from non-MALDI grade material.
[b]Non-MALDI grade material used directly without further purification.
[c]Calculations based on the assumption that $\alpha_0 = \alpha_1 = \alpha_{0s} = \alpha_{1s} = 2 \times 10^{-17}$ cm^2.

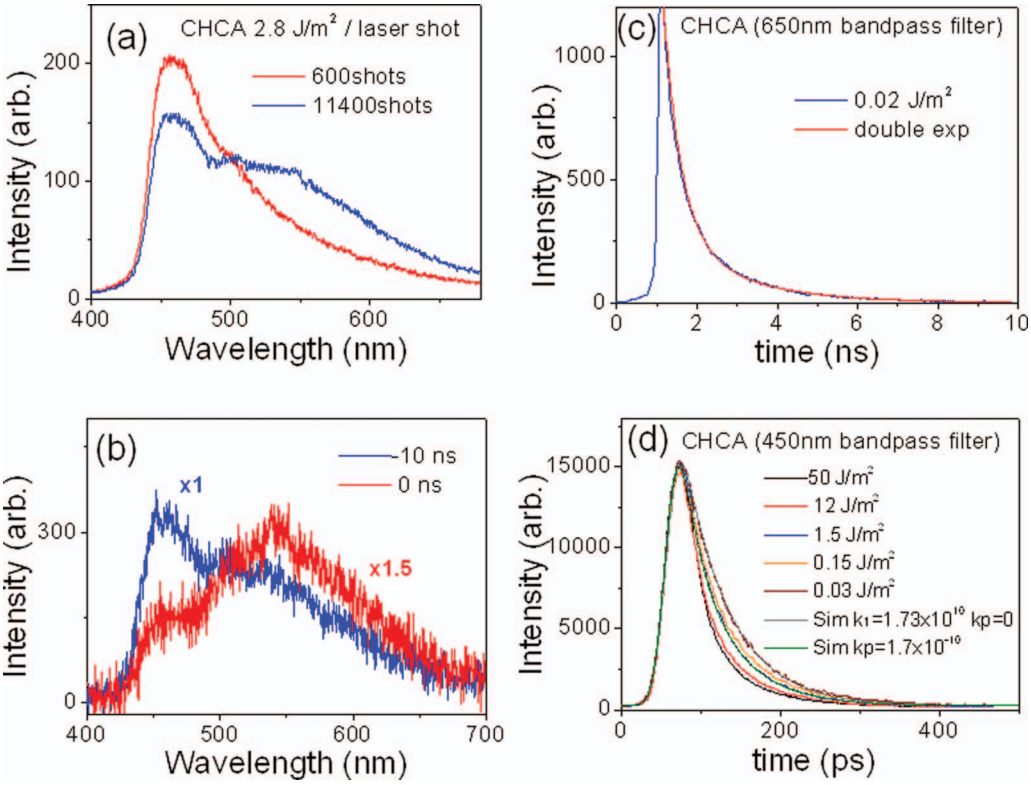

FIG. 4. Fluorescence spectra of CHCA. (a) Obtained using a spectrograph and ICCD after illumination by 600 and 11400 laser shots. The time-gated window of the ICCD was opened 10 ns before the excitation laser pulse arrived, and it remained open for 100 ns. (b) Obtained using a spectrograph and ICCD. The time-gated window of the ICCD was opened −10 and 0 ns before the excitation laser pulse (5 ns pulse width) arrived, and it remained open for 10 ns. (c) and (d) Time-resolved fluorescence intensity using a 20-ps laser pulse and streak camera for excitation and detection, respectively. An additional filter (650 nm bandpass filter for (c) and 450 nm shortpass filter for (d)) was placed in front of the streak camera.

S_0 state. Dimers were produced from the reaction between the C–C double bonds in the long chain of each monomer. It has a structure containing a four-membered ring. Because the laser fluence was considerably low, no desorption occurred. A growing dimer concentration was observed upon continuous illumination. Lifetime of the monomer and dimer was 34 ± 15 ps and 1–2 ns, respectively.

We observed the similar change of fluorescence spectra reported by Hoyer *et al.* Figure 4(a) shows that continual illumination with 355 nm photons caused a growing band centered at 550 nm. We found that the relative intensity of the 550 nm band for a given number of laser shot decreased as the laser fluence (per laser shot) increased. We offer two possible explanations for the decrease of 550 nm band at high laser fluences. First, low laser fluences resulted in photodimer accumulation in the solid state. As the laser fluence increased, the molecules (i.e., both monomers and dimers) desorbed from the solid state, and only the newly formed dimers in the same laser shot contributed to the spectra at 550 nm. Second, multiphoton absorption and S_1-S_1 annihilation competed with the photodimerization reaction at high laser fluences.

Figure 4(b) shows the time-resolved fluorescence spectra. The relative intensities of spectrum in the region 400–500 nm and spectrum in the region 500–700 nm change with the observation time window. To measure the lifetime of these two components, we placed an additional filter (450 nm 450FS40-25, or 650 nm 650FS40-25 bandpass filter, Andover, NH, USA) in front of the streak camera to reduce interference from the other component. The lifetime of the slow component (dimmer) is 1.7 ns, as shown in Figure 4(c). Figure 4(d) shows that the fluorescence intensity of the fast component (monomer) can be expressed as a single exponential function of an excited-state lifetime $\tau = 1/k_1 = 57.8$ ps at low laser fluence (0.03 J/m^2). The excited-state lifetime of monomers observed in this study (57.8 ps) and those reported by Hoyer *et al.*[26] (35 ± 15 ps) was considerably shorter than the lifetime (1.8 ns) that Knochenmuss applied in his recent simulation.[28]

Figure 4(d) shows that the excited-state lifetime decreased as the laser fluence increased. Allwood *et al.*[25] reported that the α_0 value of solid CHCA was 6.8×10^{-17} cm^2. Our numerical simulation (used the value of α_0 reported by Allwood *et al.*) fitted to the experimental data at laser fluence (1.5 J/m^2) showed that the value of k_2 was 1.7×10^{-10} cm^3 molecule^{-1} s^{-1}, which is similar to that of 2,5-DHB. The values of k_1 and k_2 from non-MALDI grade material are close to the values of MALDI grade material.

3. Sinapinic acid (SA)

Hoyer *et al.* reported the change of fluorescence spectra of sinapinic acid (SA) after illumination by 325 nm photons.[26,27] The initial fluorescence spectra of SA exhibited a broad band from 420 to 700 nm, and the maximum intensity was observed at 490 nm. After the illumination by 325 nm photons, the fluorescence spectra exhibited an additional broad band from 420 to 700 nm which the maximum

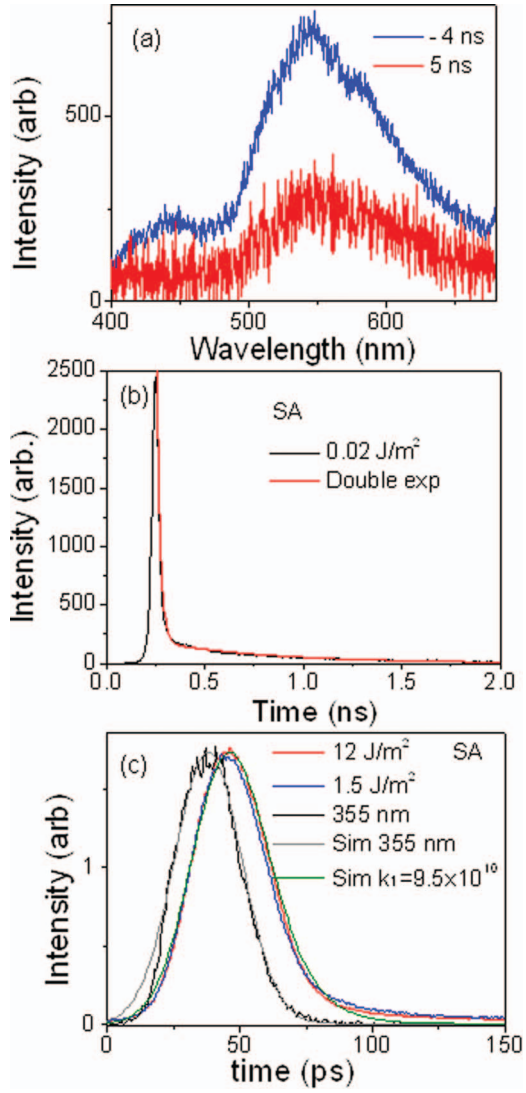

FIG. 5. (a) Fluorescence spectra of SA obtained using a spectrograph and ICCD. The time-gated window of the ICCD was opened 4 ns before the excitation laser pulse arrived or 5 ns after the excitation laser pulse arrived, and remained open for 10 ns. (b) and (c) Time-resolved fluorescence intensity using a 20-ps laser pulse and streak camera for excitation and detection, respectively. An additional filter (450 nm bandpass filter) was placed in front of the camera for (c).

intensity was observed at 550 nm. Similar to the CHCA observations, the additional broad band was attributed to fluorescence from photodimers. The lifetime of the excited-state dimers was long (1–2 ns), whereas that of the excited-state monomers was too short to measure using picosecond laser pulses and time-correlated single-photon counting techniques.[27] The lifetime of the excited-state monomers was determined to be 400 ± 100 fs using the techniques of two-photon femtosecond excitation at 800 nm.[26]

We observed the similar change of fluorescence spectra to those reported by Hoyer *et al.* A growing band centered at 550 nm was observed when the SA was continually illuminated with 355-nm photons. Figure 5(a) shows that the time-resolved fluorescence spectra comprise fast and slow components. The spectra in the region 400–500 nm were not observed in long delay time. Figure 5(b) shows the fluorescence intensity decay curve can be described by two lifetimes. The lifetime of the slow component was 0.6 ns. To measure the excited state lifetime of the fast component, we placed an additional filter (450 nm) in front of the streak camera to minimize interference from the other component. Figure 5(c) shows the k_1 was 9.5×10^{10} s^{-1}, corresponding to a lifetime was 10.5 ps for the fast component. However, we were unable to determine the value of k_2 because of the ultra-short excited-state lifetime. Although S_1-S_1 annihilation of SA cannot be determined based on the fluorescence intensity decay, the short lifetime indicates that most molecules in the S_1 state decay through internal conversion and fluorescence emission. If S_1-S_1 annihilation occurs in SA, its efficiency is considerably less than that of 2,5DHB (assuming that they have an identical k_2 value). The non-MALDI grade material shows similar results.

4. 3-Hydroxy-picolinic acid (3-HPA)

In this study, the 3-HPA fluorescence properties were similar to those of CHCA and SA. An additional band centered at 510 nm was observed at low laser fluences, and this band increased in conjunction with the number of laser shots. Figure 6(a) shows that the relative intensity of the additional band decreased as the laser fluence increased. This band was attributed to reaction products of the 355 nm photons. Figure 6(b) shows that the fluorescence spectra of the reaction products ranged from 450 to 660 nm. To measure the lifetime of these products, we placed an additional filter (550-nm bandpass filter, 550FS40-25, Andover, NH, USA) in front of the streak camera to enhance the relative fluorescence intensity of the photoproducts. The results shown in Figure 6(c) indicate that the excited-state lifetime of the reaction products was 2.2 ns.

To measure the time-resolved fluorescence of the excited-state monomers, we placed an additional filter (450 nm short-pass filter) in front of the streak camera to minimize interference from the fluorescence of the reaction products. The results shown in Figure 6(d) indicate that increasing the laser fluence exerted no effect on the fluorescence lifetime of 3-HPA (83 ps), thereby indicating that no S_1-S_1 annihilation occurred. The upper limit of k_2 was obtained by comparing the simulation and experimental measurements at the highest level of laser fluence. Based on the assumption that $\alpha_0 = \alpha_1 = \alpha_{0s} = \alpha_{1s} = 2 \times 10^{-17}$ cm^2 (similar to the absorption cross sections of 2,5-DHB, FA, and SA), the estimated upper limit of S_1-S_1 annihilation rate constant was 5×10^{-13} cm^3 $molecule^{-1}$ s^{-1}. The value of k_2 was not sensitive to α_1, α_{0s}, and α_{1s}, although it was sensitive to α_0. When α_0 increased by a factor of three, the upper limit of k_2 decreased by a factor of approximately two.

A previous study argued that a decrease in fluorescence quantum yield of 3-HPA as the laser fluence increases is evidence of S_1-S_1 annihilation.[14] However, that study did not consider the formation of photoproducts. As shown in Figure 6(b), the relative concentration of photoproducts decreased as the laser fluence increased. Therefore, in addition to the multiphoton absorption, we can attribute the decrease in fluorescence quantum yield (as the laser fluence increased)

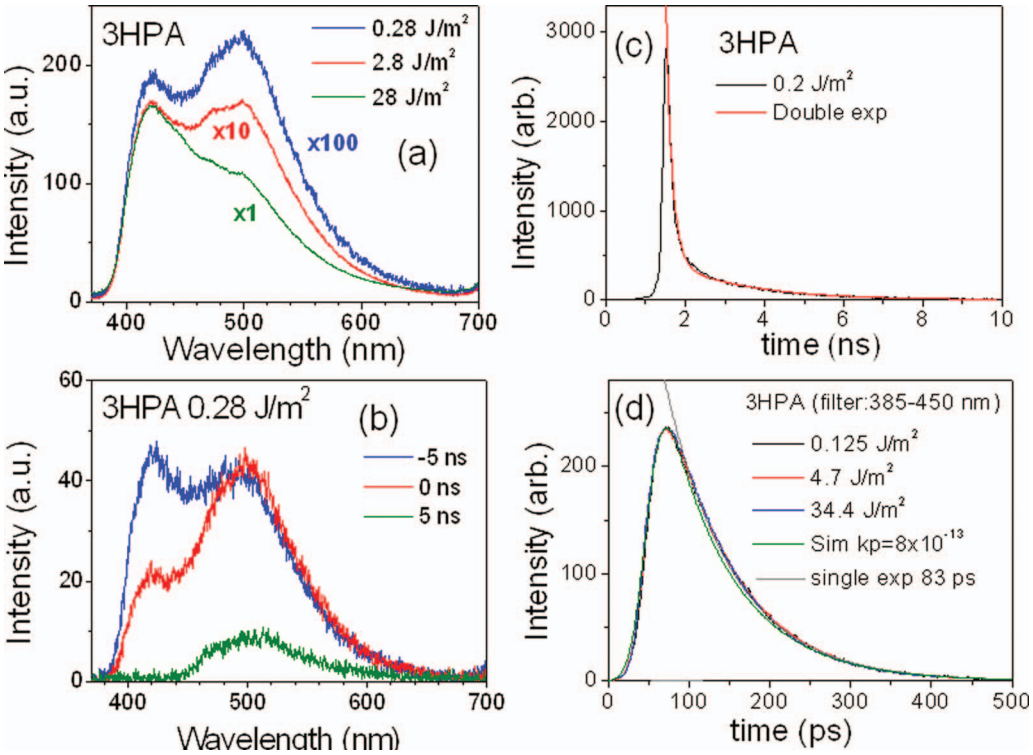

FIG. 6. Fluorescence spectra of 3-HPA (a) obtained from a spectrograph and ICCD at various laser fluences (355 nm, 5 ns pulse width). The time-gated window of the ICCD was opened 10 ns before the excitation laser pulse arrived, and it remained open for 100 ns. (b) Fluorescence spectra obtained using a spectrograph and ICCD. The time-gated window of the ICCD was opened −5, 0, and 5 ns before the excitation laser pulse (5 ns pulse width) arrived, and it remained open for 10 ns. (c) and (d) Time-resolved fluorescence intensity was measured using a 20-ps laser pulse and recorded using streak camera. An additional filter (550 nm bandpass filter for (c) and 450 nm short pass filter for (d)) was placed in front of the camera.

to the generation of photoproducts if the fluorescence quantum yield of the photoproducts is greater than that of the monomers.

5. 6-Aza-2-thiothymine (ATT)

Figure 7(a) shows that the time-resolved fluorescence intensity profiles of 6-aza-2-thiothymine were unaffected by changes in laser fluence, indicating that S_1-S_1 annihilation did not occur. The excited-state lifetime of ATT was 52 ps ($k_1 = 1.9 \times 10^{10}$ s^{-1}), and the upper limit of k_2 was 6×10^{-12} cm^3 molecule^{-1} s^{-1}. We attributed the markedly higher k_2 upper limit to the short lifetime of excited-state ATT.

6. 2,4-Dihydroxy-acetophenone (2,4-DHAP)

Figure 7(b) shows that the excited-state lifetime (1.1 ns) of 2,4-DHAP remained constant as the laser fluence increased from 0.024 to 63 J/m^2. The simulation results fitted to the highest laser fluence level indicate that the upper limit of the S_1-S_1 annihilation rate constant is k_2 is 3×10^{-14} cm^3 molecule^{-1} s^{-1}, which is approximately 5000-fold less than that of 2,5-DHB. The non-MALDI grade material has similar results.

7. 2,5-Dihydroxy-acetophenone (2,5-DHAP)

Figure 7(c) shows that minor changes occurred in the excited-state lifetime (279 ps) of 2,5-DHAP as the laser fluence increased from 0.14 to 26.5 J/m^2. The fluorescence simulation results show that k_2 is 6×10^{-12} cm^3 molecule^{-1} s^{-1} when the laser fluence is 6.1 J/m^2.

8. 2,6-Dihydroxy-acetophenone (2,6-DHAP)

Figure 8(a) shows the fluorescence intensity decays at various laser fluence levels. At the lowest laser fluence level (0.00067 J/m^2), the intensity decay fits the sum of two exponential decays (Eq. (5)) exhibiting 54- and 305-ps lifetimes:

$$\frac{d[S_1(t)]}{dt} = -C_1 k_1 [S_1(t)] - C_2 k_2 [S_1(t)]. \quad (5)$$

The laser fluence at 0.00067 J/m^2 corresponded to a laser intensity of 3.3×10^7 J m^{-2} s^{-1}. At such low laser intensity, the probability of multiphoton absorption or S_1-S_1 annihilation occurring is low. The presence of two lifetimes in the fluorescence intensity decay at low laser fluences indicates the existence of two electronically excited states that exhibit similar energy levels; however, the energy levels of these states were too close to clearly observe two separate bands in the fluorescence spectra.

The time-resolved fluorescence intensity profiles remained constant when the laser fluence ranged from 0.00067 to 23.4 J/m^2, indicating that S_1-S_1 annihilation did not occur. Although the fluorescence intensity decayed considerably faster at high laser fluences (57–394 J/m^2) than it did at low fluences, the intensity profile fit to the sum of two exponential

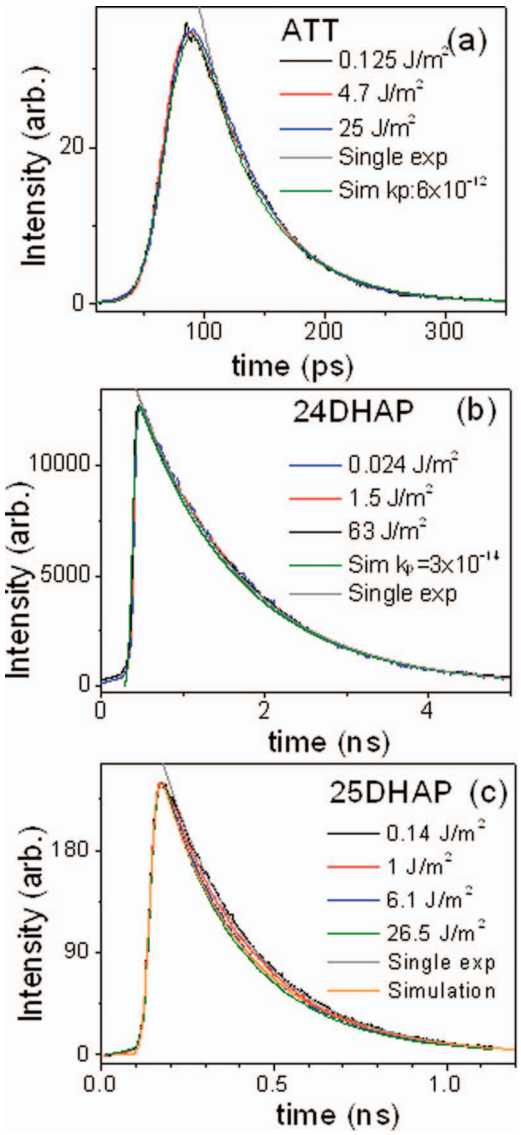

FIG. 7. Time-resolved fluorescence intensity using a 20 ps laser pulse and streak camera for excitation and detection, respectively. (a) ATT, (b) 2,4-DHAP, and (c) 2,5-DHAP.

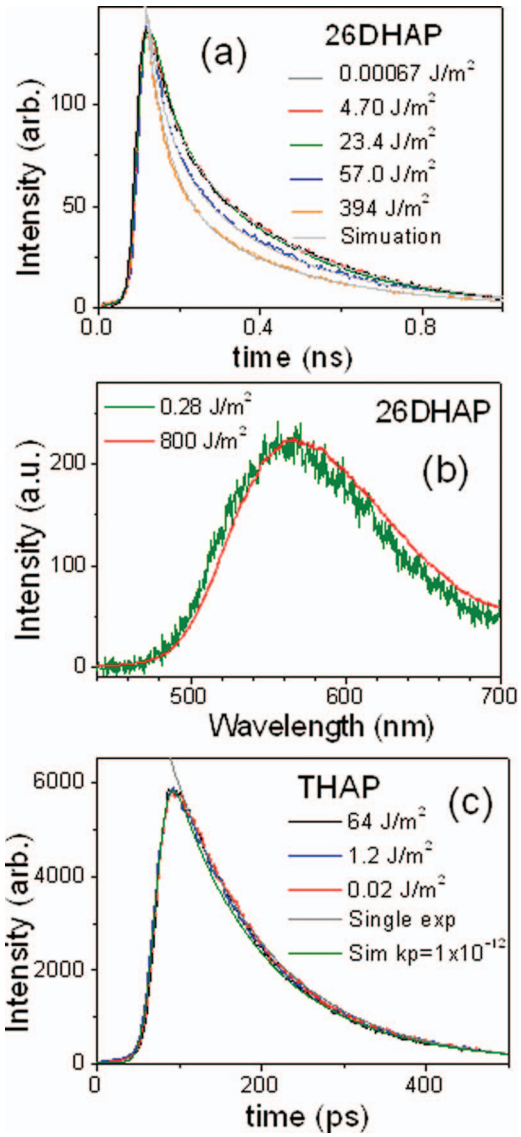

FIG. 8. (a) Time-resolved fluorescence intensity of 2,6-DHAP. A 20 ps laser pulse and streak camera were used for excitation and recording, respectively. (b) Fluorescence spectra of 2,6-DHAP were obtained using a spectrograph and ICCD at various laser fluences (355 nm, 5 ns pulse width). (c) Time-resolved fluorescence intensity of THAP. A 20 ps laser pulse and streak camera were used for excitation and recording, respectively.

decays that exhibited identical lifetimes but distinct amplitude ratios. As shown in Eq. (5), the amplitude C_1 (C_2), which denotes the amplitude of a short (long) lifetime, increased from 50 (100) at a low laser fluence to 70 (80) at 57 J/m^2, and then increased further to 89.5 (60.5) when the laser fluence was 394 J/m^2. These changes might be attributed to (1) the complete saturation of one transition before saturation occurred in the other transition, or (2) one electronically excited state has a larger absorption cross section, α_1, than the other, resulting in a large probability of multiphoton absorption, or (3) formation of photoproducts analogous to that of CHCA, SA, and 3-HPA. These possibilities can result in the changes in the fluorescence spectrum at various laser fluences, as shown in Figure 8(b). A small red shift was observed at high laser fluence, indicating that (1) the fluorescence spectrum of the saturated transition red-shifted to the fluorescence spectrum of the other transition, or (2) the electronically excited state corresponding to the blue-shifted fluorescence spectrum has a larger absorption cross section than the other electronically excited state, or (3) fluorescence spectrum of photoproducts blue-shifted to the fluorescence spectrum of monomers.

9. 2,4,6-Trihydroxy-acetophenone (THAP)

The excited state lifetime of THAP at low laser fluence was found to be $1/k_l = 120$ ps. S_1-S_1 annihilation was not observed in THAP, as shown in Figure 8(c). Simulation shows that the upper limit of S_1-S_1 annihilation rate constant is 1×10^{-12} cm^3 molecule^{-1} s^{-1}. The lifetime of non-MALDI grade material depended on the length of time that the crystals were in the vacuum. Initially, the lifetime was 110 ps, and no change was observed during the first 16 min in vacuum. Subsequently, the lifetime gradually increased to 147 ps at

70 min, and then 175 ps at 4 h. No energy pooling was observed in non-MALDI grade THAP, in both air and a vacuum.

B. Other matrices

1. Ferulic acid (FA)

FA is a commonly used matrix in MALDI, although it was not listed as such by Hillenkamp and Karas.[22] According to previous research,[25] FA is one of four matrices in which the absorption cross section has been measured in the solid state (the other three matrices are 2,5-DHB, CHCA, and SA). Therefore, we can calculate the rate constant k_2 based on the reported absorption cross-section values. Figure 9(a) shows the lifetime remained constant at 104 ps, regardless of any changes in laser fluence. A previous study[25] reported that the absorption cross section of solid state FA is 1.25×10^5 cm^{-1} or 3.14×10^{-17} cm^2 for a density of 1.28 g/cm^3. The upper limit of S_1-S_1 annihilation rate constant was 2×10^{-13} cm^3 molecule^{-1} s^{-1} when $\alpha_1 = \alpha_{0s} = \alpha_{1s} = 3.14 \times 10^{-17}$ cm^2. The upper limit of k_2 was approximately 800-fold less than that of 2,5-DHB.The non-MALDI grade material has similar results.

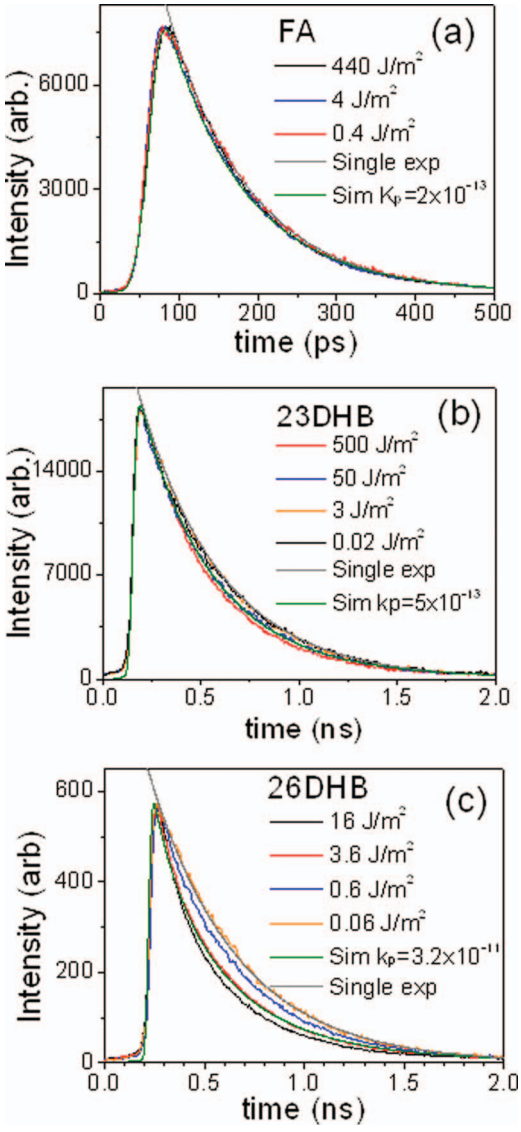

FIG. 9. Time-resolved fluorescence intensity using a 20-ps laser pulse and streak camera for excitation and detection, respectively. (a) FA, (b) 2,3-DHB, and (c) 2,6-DHB.

2. DHB isomers

Among the six positional isomers of dihydroxybenzoic acid (DHB), 2,5-DHB is more favorable than the other isomers when used as matrix in MALDI because more ions can be generated using 2,5-DHB at 337 and 355 nm. The numbers of analyte ions generated from the matrices of the other positional isomers at 355 nm are either extremely low or nonexistent. Numerous studies have been conducted to determine why 2,5-DHB is superior to other isomers.[23,29–35] A recent study showed that 2,5-DHB is not the optimal matrix if the laser wavelength is set at 322 nm at which the neutral desorption of DHB isomers is similar.[23] Compared with 2,4-DHB and 2,5DHB at the wavelength of 322 nm, 2,3-DHB and 2,6-DHB generate more ions. In this study, we investigated the S_1-S_1 annihilation of these isomers and searched for the possible correlation between S_1-S_1 annihilation and ion generation efficiencies among these isomers.

3. 2,3-Dihydroxybenzoic acid (2,3-DHB)

Figure 9(b) shows that no change of fluorescence lifetime occurred, as the laser fluence increased from 0.02 to 3 J/m^2. This is in the similar peak power region of nanosecond laser pulses in MALDI. The experimental measurement results fit a single exponential decay with a lifetime of 400 ps. A small change of fluorescence lifetime was observed only in very large laser fluences (50–500 J/m^2) region. The simulation results show that k_2 is 5×10^{-13} cm^3 molecule^{-1} s^{-1}, which is 320-fold less than that of 2,5-DHB. The rate constant k_2 of 2,3-DHB is very small such that it is close or smaller than the upper limit of k_2 of the other matrices which S_1-S_1 annihilation does not occur. No S_1-S_1 annihilation was observed for the non-MALDI grade material and k_1 is similar to that of MALDI grade material.

4. 2,6-Dihydroxybenzoic acid (2,6-DHB)

Figure 9(c) shows that the experimental measurement results at low laser fluences (0.06 J/m^2) fit a single exponential decay exhibiting a lifetime of 465 ps, and fitting the simulation results to the experimental measurements at 3.6 J/m^2 indicated that $k_2 = 3.2 \times 10^{-11}$ cm^3 molecule^{-1} s^{-1}. The k_1 and k_2 of non-MALDI grade material are in the similar order of magnitudes to that of MALDI grade material.

C. Implications of the MALDI mechanisms

Typical MALDI sample contains matrix and analyte. However, pure matrix was frequently used in theoretical models and experimental studies to investigate the ionization mechanism of MALDI. For example, Ehring *et al.* studied the fluorescence quantum yields of pure 2,5-DHB matrix and suggested the relation between S_1-S_1 annihilation and MALDI

mechanism.[13] Hillenkamp and co-workers extended Ehring's study using three pure matrices.[14] Knochenmuss used energy pooling model to predict the MALDI properties of pure 2,5-DHB matrix.[7] He cited the works by Ehring *et al.* and by Hillenkamp *et al.* (which were conducted using pure matrix) as the evidence to support his energy pooling model.

Trimpin *et al.* used solvent-free MALDI (i.e., the matrix and analyte crystals were separately ground into powder, then the samples were prepared by mixing the matrix and analyte powders directly without using solvent) and showed that the MALDI performance was inversely proportional to crystal size, indicating that surface contact between analyte and matrix was crucial but the incorporation of analyte into the matrix crystals was not necessary.[31] Many studies also used this solvent-free method in MALDI sample preparation.[36–38] Kim *et al.* showed that the total number of ions generation from pure matrix was found to be the same as the total number of ions generated from the sample containing analyte with a typical analyte to matrix molar ratio (less than 0.1%).[38,39] All of the studies described above suggest that the pure matrix crystals contain the most important properties related to MALDI ionization mechanism. This is particularly true when S_1-S_1 annihilation is investigated. The impurity (one possible "impurity" is analyte) in matrix has little effects on S_1-S_1 annihilation, as shown in the comparison of MALDI grade and non-MALDI grade materials in this work for the existence of impurity and in the study by Lu *et al.*[38] for the existence of analyte, or the impurity decreases the S_1-S_1 annihilation efficiency, as shown by Setz and Knochenmuss.[40] It is not likely that the existence of analyte in matrix crystal can enhance the S_1-S_1 annihilation. No such enhancement has been reported. Therefore, the study of S_1-S_1 annihilation using pure matrix crystals provides the necessary information to justify the role of S_1-S_1 annihilation in MALDI ionization mechanism.

The investigation of S_1-S_1 annihilation based on the time-resolved fluorescence for 12 matrices shows that S_1-S_1 annihilation was not observed in 6 matrices, namely 3-HPA, ATT, 2,4-DHAP, 2,6-DHAP, THAP, and FA. Reactions between two matrix molecules in electronically excited states were observed in only 5 matrices (2,5-DHB, CHCA, 2,5-DHAP, 2,3-DHB, 2,6-DHB,), and S_1-S_1 annihilation could be responsible for one of these reactions. For the matrices which S_1-S_1 annihilation was not observed in pure matrices, S_1-S_1 annihilation is not likely to occur in the mixture of matrix and analyte. Thus, the results indicate that S_1-S_1 annihilation is unnecessary in MALDI process.

Comparing the matrix activity among the DHB isomers shows that the ion-generation efficiency of both 2,3-DHB and 2,6-DHB is superior to that of 2,4-DHB and 2,5-DHB when the excitation laser wavelength is set at 322 nm such that these three isomers have similar desorbed neutral molecules.[33] At this wavelength, the ion intensity generated from 2,5-DHB is approximately 10-fold less than that of 2,3-DHB and 2,6-DHB.

Because of the high collision frequency between molecules in the condensed phase, vibrational energy relaxation is extremely rapid. Molecules excited with 322 or 355 nm photons rapidly relax to the low vibrational energy levels in the S_1 state. If S_1-S_1 annihilation occurs, it occurs within these low vibrational energy levels, regardless of the initial excitation laser wavelength. Consequently, the S_1-S_1 annihilation rate constant observed in this study (using 355-nm photons) can be applied to molecules excited with 322-nm photons. Although 2,3-DHB and 2,6-DHB are superior matrices at 322 nm, the results of this study indicate that the S_1-S_1 annihilation rate constant of 2,3-DHB and 2,6-DHB is 320 and 5 times less than that of 2,5-DHB, respectively. No correlation was observed between the ion-generation efficiency and S_1-S_1 annihilation rate constant. Thus the findings suggest that S_1-S_1 annihilation is not crucial in the ionization mechanism in MALDI.

Thermal proton transfer model has been proposed to explain the primary ion generation in MALDI.[12] Absolute absorption cross section of solid state matrix was used in this model to predict the temperature after laser irradiation. The predicted temperature and heat of proton transfer reaction were used to calculate the ion generation efficiency (ion-to-neutral ratio). Temperature is the dominate factor in the determination of ion generation efficiency for similar heat of proton transfer reaction. The absolute absorption cross section of solid state matrix is available only for four matrices,[25] namely 2,5-DHB, CHCA, SA, and FA. The absorption cross section at 355 nm was found to be in the sequence CHCA $\gg$ FA = SA $>$ 2,5-DHB. Recent study showed that the sequence of ion generation efficiency was similar to that of absorption cross section sequence,[41,42] indicating that thermal proton transfer plays a crucial role in MALDI ionization mechanism.

Although we showed that many matrices do not undergo the S_1-S_1 annihilation, the possibility of T_1-T_1 annihilation for these molecules is not excluded. In particularly, molecules containing carbonyl functional group (DHAP and THAP) may have large probability to undergo intersystem crossing. However, current energy pooling model described the ion generation through S_1-S_1 annihilation. If energy pooling plays a crucial role in MALDI ion generation, modification of the current model is necessary. Investigations of the T_1-T_1 annihilation for the molecules which do not undergo S_1-S_1 annihilation and the possibility of ion generation from T_1-T_1 annihilation are interesting for the future theoretical development of MALDI.

ACKNOWLEDGMENTS

We acknowledge the support from the Thematic Research Program of the Academia Sinica, Taiwan (As-102-TP-A08) and the National Science Council of Taiwan (NSC100-2113-M-011-026-MY3).

[1] K. Tanaka, H. Waki, Y. Ido, S. Kita, and Y. Yoshida, Rapid Commun. Mass Spectrom. **2**, 151 (1988).
[2] M. Karas and F. Hillenkamp, Anal. Chem. **60**, 2299 (1988).
[3] M. Karas, D. Bachmann, U. Bahr, and F. Hillenkamp, Int. J. Mass Spectrom. Ion Processes **78**, 53 (1987).
[4] H. Ehring, M. Karas, and F. Hillenkamp, Org. Mass Spectrom. **27**, 472 (1992).
[5] M. Karas, M. Gluckmann, and J. Schafer, J. Mass Spectrom. **35**, 1 (2000).
[6] D. A. Allwood, P. E. Dyer, and R. W. Dreyfus, Rapid Commun. Mass Spectrom. **11**, 499 (1997).
[7] R. Knochenmuss, J. Mass Spectrom. **37**, 867 (2002).

[8]R. Knochenmuss, Anal. Chem. **75**, 2199 (2003).
[9]X. Chen, J. A. Carroll, and R. C. Beavis, J. Am. Soc. Mass Spectrom. **9**, 885 (1998).
[10]S. Niu, W. Zhang, and B. T. Chait, J. Am. Soc. Mass Spectrom. **9**, 1 (1998).
[11]Y. H. Lai, C. C. Wang, S. H. Lin, Y. T. Lee, and Y. S. Wang, J. Phys. Chem. B **114**, 13847 (2010).
[12]K. Y. Chu, S. Lee, M. T. Tsai, I. C. Lu, Y. A. Dyakov, Y. H. Lai, Y. T. Lee, and C. K. Ni, J. Am. Soc. Mass Spectrom. **25**, 310 (2014); **25**, 1087 (2014).
[13]H. Ehring and B. U. R. Sundqvist, J. Mass Spectrom. **30**, 1303 (1995).
[14]H. C. Ludemann, R. W. Redmond, and F. Hillenkamp, Rapid Commun. Mass Spectrom. **16**, 1287 (2002).
[15]M. T. Tsai, S. Lee, I. C. Lu, K. Y. Chu, C. W. Liang, C. H. Lee, Y. T. Lee, and C. K. Ni, Rapid Commun. Mass Spectrom. **27**, 955 (2013).
[16]A. P. Quist, T. Huth-Fehre, and B. U. R. Sundqvist, Rapid Commun. Mass Spectrom. **8**, 149 (1994).
[17]Y. J. Bae, Y. S. Shin, J. H. Moon, and M. S. Kim, J. Am. Soc. Mass Spectrom. **23**, 1326 (2012).
[18]K. M. Park, S. H. Ahn, Y. J. Bae, and M. S. Kim, Bull. Korean Chem. Soc. **34**, 907 (2013).
[19]A. A. Puretzky and D. B. Geohegan, Chem. Phys. Lett. **286**, 425 (1998).
[20]M. Klessinger and M. Michl, *Excited States and Photochemistry of Organic Molecules* (VCH Publishers, Inc., New York, 1995), p. 295.
[21]H. Y. Lin, B. T. Song, I. C. Lu, K. T. Hsu, C. Y. Liao, Y. Y. Lee, C. M. Tseng, Y. T. Lee, and C. K. Ni, Rapid Commun. Mass Spectrom. **28**, 77 (2014).
[22]F. Hillenkamp and M. Karas, in *MALDI MS A Practical Guide to Instrumentation Methods and Applications*, edited by F. Hillenkamp and J. Peter-Katalinic (WILEY-VCH Verlag GmbH & Co. KGaA, Weinheim, 2007), p. 19.
[23]C. W. Liang, C. H. Lee, Y. J. Lin, Y. T. Lee, and C. K. Ni, J. Phys. Chem. B **117**, 5058 (2013).
[24]See supplementary material at http://dx.doi.org/10.1063/1.4898372 for the details of materials and the plots of logarithm of fluorescence intensity verse time.
[25]D. A. Allwood, R. W. Dreyfus, I. K. Perera, and P. E. Dyer, Rapid Commun. Mass Spectrom. **10**, 1575 (1996).
[26]T. Hoyer, W. Tuszynski, and C. Lienau, Chem. Phys. Lett. **443**, 107 (2007).
[27]T. Hoyer, W. Tuszynski, and C. Lienau, Phys. Chem. Chem. Phys. **12**, 13052 (2010).
[28]R. Knochenmuss, Analyst **139**, 147 (2014).
[29]D. M. Price, S. Bashir, and P. R. Derrick, Thermochim. Acta **327**, 167 (1999).
[30]V. Horneffer, K. Dreisewerd, H. C. Ludemann, F. Hillenkamp, M. Lage, and K. Strupat, Int. J. Mass Spectrom. **185–187**, 859 (1999).
[31]S. Trimpin, H. J. Rader, and K. Mullen, Int. J. Mass Spectrom. **253**, 13 (2006).
[32]L. Jessome, N. Y. Hsu, Y. S. Wang, and C. H. Chen, Rapid Commun. Mass Spectrom. **22**, 130 (2008).
[33]D. J. Harvey, Rapid Commun. Mass Spectrom. **7**, 614 (1993).
[34]D. J. Harvey, Mass Spectrom. Rev. **28**, 273 (2009).
[35]H. C. Hsu, I. C. Lu, P. H. Lin, Y. A. Dyakov, A. Bagchi, C. Y. Lin, S. W. Hung, Y. T. Lee, and C. K. Ni, Rapid Commun. Mass Spectrom. **28**, 1082 (2014).
[36]G. R. Kinsel, D. Yao, F. H. Yassin, and D. S. Marynick, Eur. J. Mass Spectrom. **12**, 359 (2006).
[37]C. M. Land and G. R. Kinsel, J. Am. Soc. Mass Spectrom. **12**, 726–731 (2001).
[38]I. C. Lu, C. Lee, H. Y. Chen, H. Y. Lin, S. W. Hung, Y. A. Dyakov, K. T. Hsu, C. Y. Liao, Y. Y. Lee, C. M. Tseng, Y. T. Lee, and C. K. Ni, J. Phys. Chem. B **118**, 413 (2014).
[39]S. H. Ahn, K. M. Park, Y. J. Bae, and M. S. Kim, J. Mass Spectrom. **48**, 299 (2013).
[40]P. D. Setz and R. Knochenmuss, J. Phys. Chem. A **109**, 4030 (2005).
[41]I. C. Lu, K. Y. Chu, C. Y. Lin, Y. A. Dyakov, H. C. Hsu, Y. T. Lee, and C. K. Ni, in *62nd ASMS Conference on Mass Spectrometry and Allied Topics* (American Society of Mass Spectrometry, Baltimore, 2014), poster 1074.
[42]I. C. Lu, K. Y. Chu, C. Y. Lin, S. Y. Wu, Y. A. Dyakov, J. L. Chen, A. Gray-Weale, Y. T. Lee, and C. K. Ni, "Ion-to-neutral ratios and thermal proton transfer in matrix-assisted laser desorption/ionization," J. Am. Soc. Mass Spectrom. (submitted).